Electronic Supplementary Information

Anti-corrosive Cellulose Nanocrystal/Carbon Nanotube Derived Zn Anode Interface for Dendrite-Free Aqueous Zn-ion Batteries

Hai Wang [a]*, Qin Zhao [b], Yue Wang [c], Junliang Lin [a], Weimin Li [b], Shun Watanabe [a]* and Xiaobo Wang [b]*

[a]: Department of Advanced Materials Science, Graduate School of Frontier Sciences, The University of Tokyo, 5-1-5 Kashiwanoha, Kashiwa, Chiba, 277-8561, Japan.

[b]: State Key Laboratory of Solid Lubrication, Lanzhou Institute of Chemical Physics, Chinese Academy of Sciences, Lanzhou730000, People's Republic of China.

[c]: Department of Electrical Engineering, Hanyang University, Seoul 04763, Republic of Korea

*Corresponding author

Email address: haiwang@edu.k.u-tokyo.ac.jp, swatanabe@edu.k.u-tokyo.ac.jp, wangxb@licp.cas.cn

Number of pages: 16

Number of figures: 8

Number of table: 2

Materials and methods

Materials. Hydrophobic cellulose nanocrystal was purchased from Suzhou Keming Biotechnology Co., LTD. Carboxylated multiwalled carbon nanotube (MWCNT) was purchased from Nanjing Xianfeng Nano. N-methyl pyrrolidone (NMP, AR) and was purchased from Aladdin Reagent (China) Co., Ltd. Ethanol was purchased from Sinopharm Chemical Reagent Co. and Polyvinylidence fluoride (PVDF, AR) was purchased from Sigma-Aldrich. Carbon black (Super P) was purchased from Alfa Aesar. Zinc sulfate heptahydrate ($ZnSO_4 \cdot 7H_2O$, AR) was bought from Sinopharm Chemical Reagent Co., Ltd., China. Zinc foil was purchased from Shenzhen AES Automation Technology Co., Ltd. Deionized water was prepared by laboratory ultrapure water machine. All the chemicals were used as received without further purification.

CNC/CNT synthesis. Cellulose nanofibers were dissolved in PMMA-acetone solution with continuous stirring for 1 hour. Then PMMA-CNC nanocristal were obtained by slow addition of ultrasonic stirring at 50 °C for several hours. CNC/CNT composites were prepared by mixing 0.528 g of MWCNT aqueous dispersion with 20 ml of distilled water containing 0.01 g of PMMA-CNC under magnetic stirring to obtain homogeneously dispersed CNC/CNT nanohybrids. The solution was poured into a glass petri dish and evaporated in an oven at 50 °C overnight and then in a vacuum oven for two days. After that, the films were peeled off from the glass plates with a spatula to obtain free-standing CNC/CNT films.

Preparation of CNC/CNT@Zn Anodes by spin-coating method

The speed was first set to 500 rpm and then the CNC/CNT solution was added dropwise as the gel spread. The speed was increased to 2000 rpm for about 30 seconds. The coated CNC/CNT@Zn anode was then dried naturally and then dried at 80°C for 5 hours to evaporate the remaining solvent. After drying in an oven at 80°C, the CNC/CNT@Zn electrode was cut into φ 14 mm circular pieces.

Preparation of V_2O_5 Cathodes

The V_2O_5 cathode was prepared in NMP solution by mixing the active material, carbon black and polyvinylidene fluoride at 8:1:1 mass ratio. The slurry is then applied to the carbon fiber using blade technology to a thickness of approximately 2 m. After drying at 100 °C for 6 hours, the electrodes were rolled and cut into 12 mm diameter discs, which were then placed in the glove box. The loading capacity of the active substance is about 2.0 mg cm^{-2}.

Zn//V_2O_5 Full Battery Assembly

Zinc/V_2O_5 full cells were assembled in an argon-filled glove box using a V_2O_5 cathode, zinc foil (or CNC/CNT@Zn) as anode, 2 M $ZnSO_4$ as electrolyte (200μL), and glass fibers (Whatman GF/D) as diaphragm. Embedded in a CR2032 coin cell. The assembled full cells were left for at least 10 hours before electrochemical testing to ensure complete wetting of the electrolyte and good electrode infusion.

Materials characterization

The surface morphology of electrodes were characterized by scanning electron microscopy (SEM, JSM 7610 plus). The micro-structures of the electrode materials were characterized using transmission electron microscopy (TEM, JEOL JEM-

2100FEG). The elemental content and crystal structure were obtained using X-ray Photoelectron Spectroscopy (XPS, Thermo Scientific ESCALAB Xi+), X-ray Diffraction (XRD, Rigaku Ultima IV) and EDS (HORIBA EMAX).

Electrochemical characterization

CR-2032 type coin cell was used for electrochemical measurements. For the coulombic efficiency (CE) test, bare Zn and CNC/CNT@Zn were fabricated into a disk with a diameter of 12 mm as the working electrode, Ti foil as the counter electrode, and glass fiber (Whatman) as the separator. The electrolyte was 2 M $ZnSO_4$ aqueous solution. The Coulombic efficiency was measured at a controlled current density of 1 mA cm^{-2} and an areal capacity of 1 mAh cm^{-2} with Zn and CNC/CNT@Zn foils as working electrodes and Cu foil as counter electrode. Electrochemical impedance spectroscopy (EIS) was performed in the frequency range of 10 mHz ~ 100 kHz. Cyclic voltammetry (CV) and constant-current charge/discharge tests (GCD) were performed on a multi-channel battery test system (Shanghai Chenhua CHI660e) for combined batteries in the voltage range of 0.2 ~ 1.6 V. The frequency range was 100 kHz ~ 1.6 V, and the frequency range was 100 kHz ~ 1.6 V. The cycling performance tests were performed on a multi-channel battery test system (ECT2001A). Electrochemical impedance spectroscopy (EIS) was performed in the frequency range of 100 kHz ~ 0.01 Hz with an amplitude of 10 mV. All electrochemical measurements and battery assemblies were performed at room temperature (25°C).

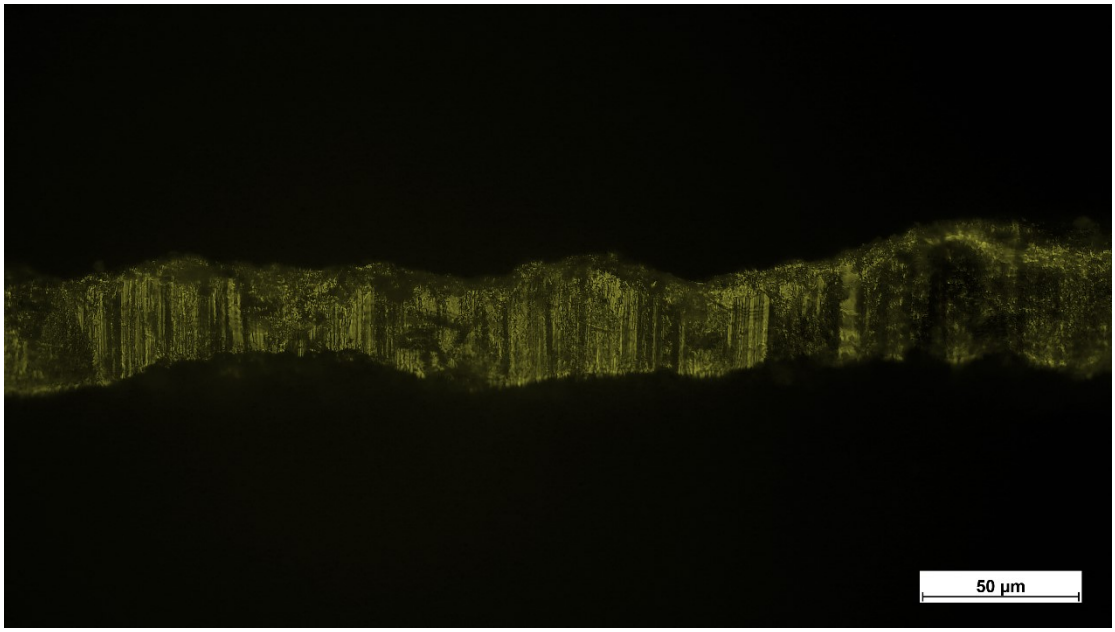

Figure S1 Corss-section image of CNC/CNT@Zn anode

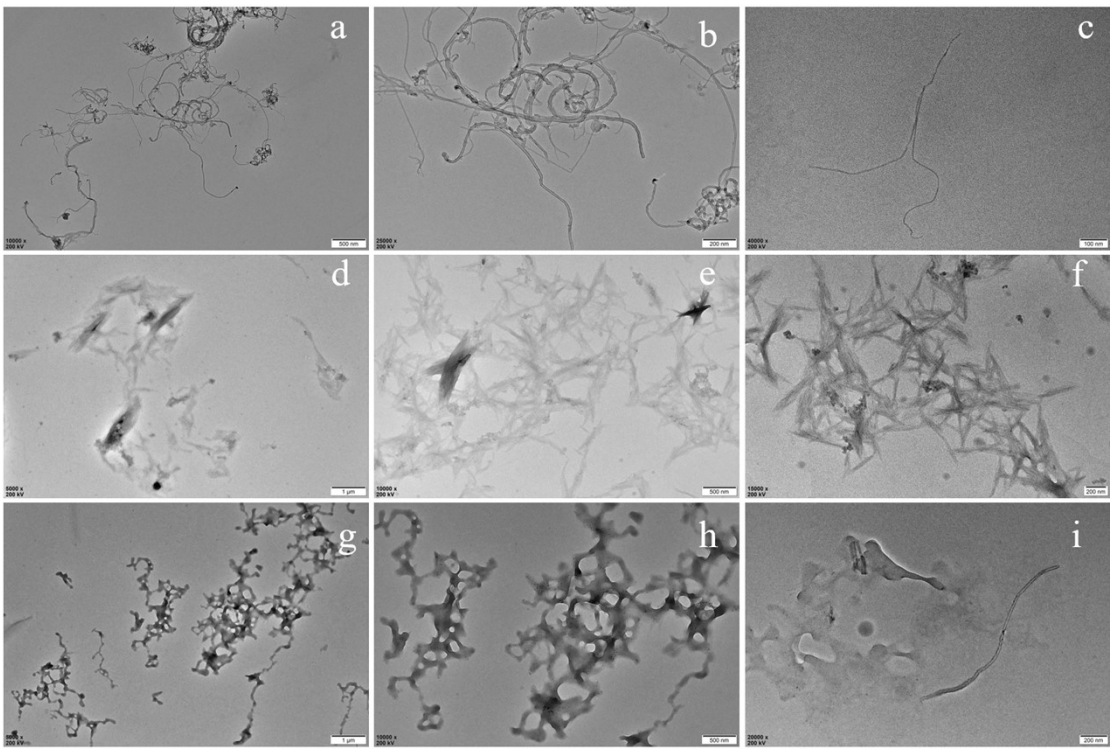

Figure S2 TEM images of (a)-(c) hydrophobic cellulose nanocrystals (CNC), (d)-(f) carbon nanotubes (CNT) and (d)-(f) CNC/CNT composite at different magnifications

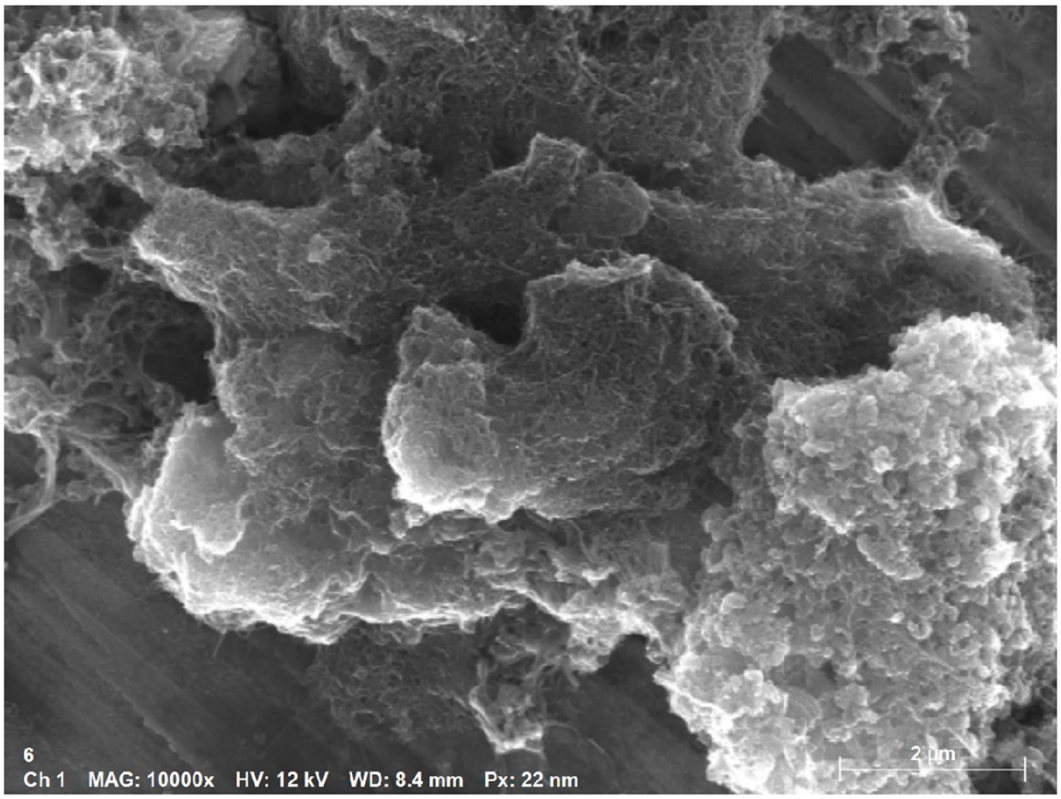

Figure S3 SEM images of the selected scan area in EDX mapping

Figure S4 Contact angle measurement of 2M $ZnSO_4$ electrolyte droplet on CNC/CNT@Zn and bare Zn anodes

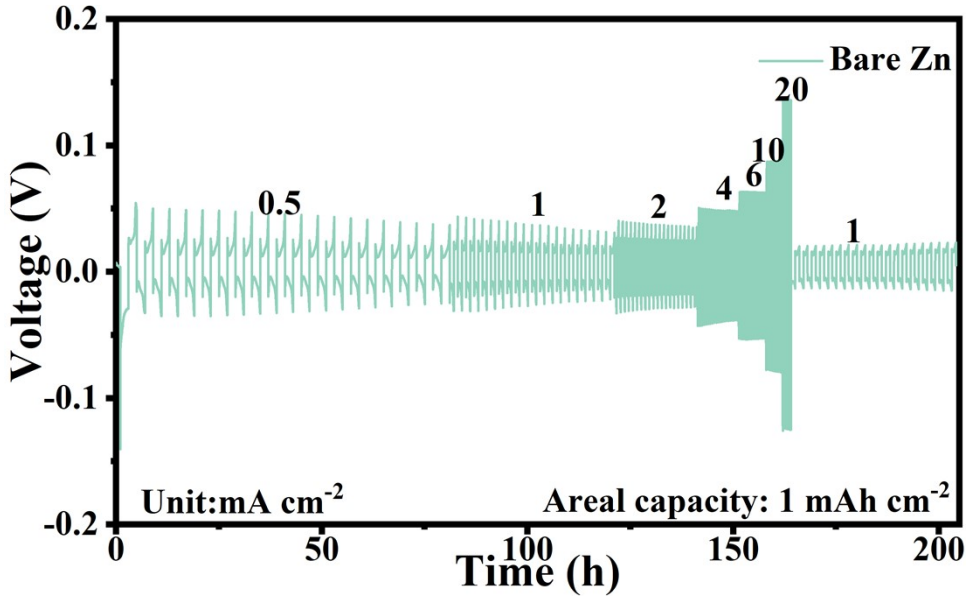

Figure S5 Rate performance of bare Zn anode

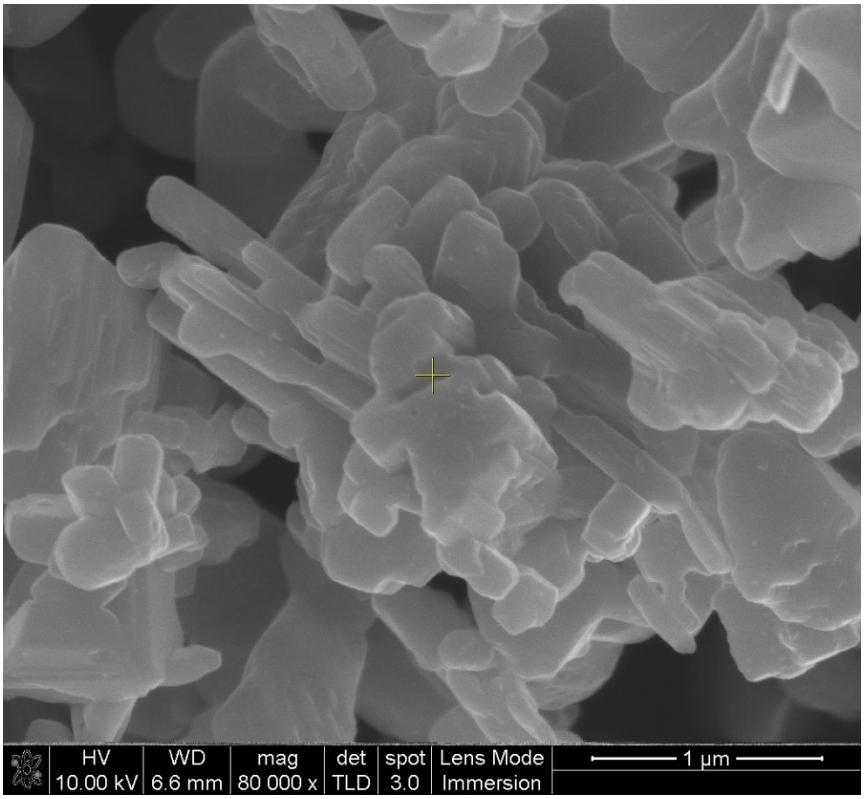

Figure S6 SEM image cathode material V_2O_5

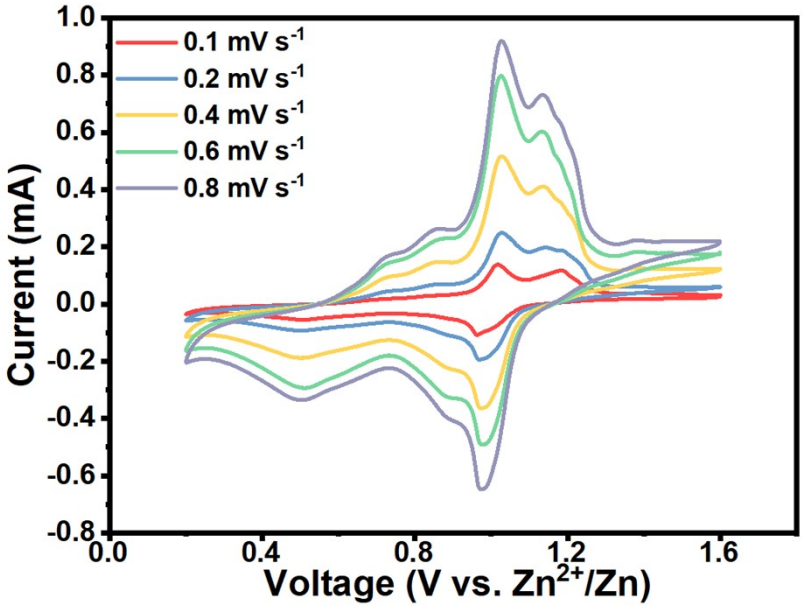

Figure S7 CV curves of CNC/CNT@Zn//V_2O_5 at various scan rate

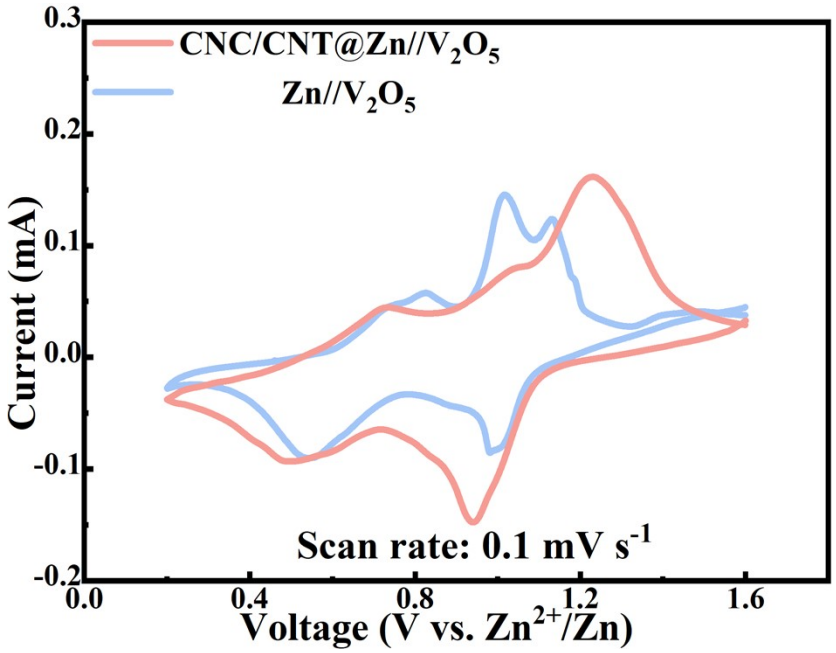

Figure S8 Comparison of CV curves of CNC/CNT@Zn//V_2O_5 and Zn//V_2O_5 full cells

Table S1. Comparison of performance for full cells from this work with reported devices

Anode	Electrolyte	Working condition (mA cm^{-2}-mAh cm^{-2})	Lifespan(h)	Reference
hmTO-Zn	3 M $Zn(CF_3SO_3)_2$	0.25-0.05	870	[1]
GFA-Zn	2 M $ZnSO_4$	3-3	700	[2]
ZA@3D-Cu	2 M $ZnBr_2$	5-5	600	[3]
PEGMA-Zn	2 M $Zn(CF_3SO_3)_2$	1-1	1100	[4]
MIL-125(Ti)-Zn	2 M $ZnSO_4$	5-5	700	[5]
Zn@ZnO	2 M $ZnSO_4$+0.1 M $MnSO_4$	3-1	1000	[6]
Zn@ZnF_2	3 M $Zn(CF_3SO_3)_2$	0.25-0.25	2000	[7]
PVB@Zn	2M $ZnSO_4$ + 0.1 M $MnSO_4$	0.2-0.2	820	[8]
GiZn	2 M $ZnSO_4$	0.1-0.1	1000	[9]
PEDOT:PSS/GS @Zn	2 M $ZnSO_4$	0.1-5	500	[10]
Zn-P-MIEC	2 M $ZnSO_4$ + 0.2 M $MnSO_4$	10-0.25	100	[11]
Zn@CNT	2 M $ZnSO_4$	5-2.5	110	[12]
GFA@Zn	2 M $ZnSO_4$	3-3	700	[13]
CNC/CNT@Zn	2 M $ZnSO_4$	5-5	750	This work

Table S2 load mass of active material and specific capacitance measured by mass ratio

Material	Active substance mass (mg)	Area (cm^{-2})	Load mass (mg cm^{-2})
V_2O_5	2.08	1.15	1.8

***Theoretical calculations**:* In this study, we performed a first-principles study to elucidate that hydrophobic cellulose/carbon nanotube enhanced the reactivity of Zn. Geometric optimization and electronic property calculations are conducted utilizing the Vienna Ab initio Simulation Package (VASP) and the Cambridge Sequential Total Energy Package (CASTEP) modules within the Materials Studio framework, grounded in the principles of Density Functional Theory (DFT).[14-15]

The Projector Augmented Plane wave method (PAW) pseudopotentials were chosen to determine the potential generalization, and the Perdew-Burke-Ernzerhof (PBE) function and the general gradient approximation (GGA) were applied to implement the exchange–correlation potential. The effects of the long-range van der Waals (vdW) corrections were treated using the Grimmes zero-damping DFT-D3 method. The energy cut-off value was set at 500 eV to ensure optimal total energy and geometric convergence requisite for the scope of this study. Brillouin zone integration was performed on grids Γ-centered 1 × 1 × 1 k-point mesh for the structural relaxation and electronic structures.[16] The energy convergence criterion was 10^{-4} eV/atom, and the maximum residual force was less than 10-2 eV/Å. The adsorption energy was calculated according to Equation S1:

$$E_{ads}=E_{total}-E_{surface}-E_{Zn} \quad \text{Equation S1}$$

where E_{ads} is the adsorption energy, E_{Total} represents the total energy of the system interacting with Zn, $E_{surface}$ is the energy of surface, E_{Zn} is the energy of the Zn.

The charge density difference can be defined according to Equation S2:

$$\Delta\rho=\rho_{total}-\rho_{base}-\rho_{Zn} \quad \text{Equation S2}$$

Where ρ_{total} represents the optimized structural charge density of the interface, ρ_{base} represents the charge density of the base that forms the CNC or CNC/CNT interface, and ρ_{Zn} represents the charge density of Zn.

Reference

1. J. Jiang , Z. Li , Z. Pan , S. Wang , Y. Chen , Q. Zhuang , Z. Ju and X. Zhang , *Energy Environ. Mater.*, 2023, **6** , e12410

2. G. Liang , J. Zhu , B. Yan , Q. Li , A. Chen , Z. Chen , X. Wang, B. Xiong , J. Fan and J. Xu , *Energy Environ. Sci.*, 2022, **15** , 1086 —1096

3. K. Xu , X. Zheng , R. Luo , J. Sun , Y. Ma , N. Chen , M. Wang , L. Song , Q. Zhao and W. Chen , *Mater. Today Energy*, 2023, **34** , 101284

4. B. Huang , J. Song , H. Kimura , Y. Li , Y. Xu , K. Yang , M. Cui , L. Du and L. Kang , *J. Power Sources*, 2023, **570** , 233048

5. C. Zhao , Y. Du , Z. Guo , A. Chen , N. Liu , X. Lu , L. Fan , Y. Zhang and N. Zhang , *Energy Stor. Mater.*, 2022, **53** , 322 —330

6. X. Xie , S. Liang , J. Gao , S. Guo , J. Guo , C. Wang, G. Xu , X. Wu , G. Chen and J. Zhou , *Energy Environ. Sci.*, 2020, **13** , 503 —510

7. Y. Yang , C. Liu , Z. Lv , H. Yang , Y. Zhang , M. Ye , L. Chen , J. Zhao and C. C. Li, *Adv. Mater.*, 2021, **33** , 2007388

8. Zhang , Q.; Liang , J.; Li , M.; Qin , J.; Zhao , Y.; Ren , L.; Liu , W.; Yang , C.; Sun , X. *Chem. Eng. J.*, 2023**, 474** , 145981

9. Y. Li , L. Wu , C. Dong , X. Wang , Y. Dong , R. He and Z. Wu , *Energy Environ. Sci.*, 2023**, 6** , e12423

10. Y. Zhang , T. Zhao , S. Yang , Y. Zhang , Y. Ma and Z. Wang, *J. Energy Chem.*, 2022, **75**, 310-320

11. M. Zhang , P. Yu , K. Xiong , Y. Wang , Y. Liu and Y. Liang , *Adv. Mater.*, 2022, **34** , 2200860

12. Y. Zeng , X. Zhang , R. Qin , X. Liu , P. Fang , D. Zheng , Y. Tong and X. Lu, *Adv. Mater.*, 2019, **31** , 1903675

13. D. Wang , Q. Li , Y. Zhao , H. Hong , H. Li, Z. Huang , G. Liang , Q. Yang and C. Zhi , *Adv. Energy Mater.*, 2022, **12** , 2102707

14. Kresse , G.; Hafner , *Phys. Rev. B*, 1993**, 47** , 558

15. S. Grimme , *J Comput. Chem.*, 2006, **27** , 1787 —1799

16. H. J. Monkhorst and J. D. Pack, *Phys. Rev. B*, 1976, **13**, 5188